Statistical Characterization of the Atmospheric Refractivity from Weather Radar Data

Rubén Nocelo López[1] and Verónica Santalla del Rio[1]

[1]*Signal Theory and Communications Department, University of Vigo, 36310 Vigo, Spain*
(Dated: 24 July 2014)

Rubén Nocelo

1. Introduction

Knowledge of temporal and spatial variations of the refractivity in the lowest part of the atmosphere is of importance in numerous fields, such as meteorology and electromagnetic wave propagation coverage prediction. In meteorology, the refractivity is used to derive temperature and humidity which is important because the convergence of moisture at low levels is related to the initiation of severe storms or deep convections (Ziegler et al., 1997). In the electromagnetic wave propagation field, the refractivity is important to predict coverages, i.e. to reduce interference between nearby stations and to ensure the required signal level within the whole coverage area, for example in White Space Devices (Selén and Kronander, 2012). Besides, knowledge of the refractivity gradient with enough temporal resolution will be of interest in the dynamic management of the spectrum. Nevertheless, the most commonly used techniques such as radiosonde launches (Viher et al., 2011), radio occultation techniques using a GPS signal (Davies et al., 2004) or the use of signals of opportunity such as Broadcast signals (Watson and Coleman, 2012) are not able to provide sufficient spatial or temporal resolution, besides they are not suitable for measuring near surface refractivity. Recently, it has been shown that refractivity can also be obtained from the radar response to stationary ground targets (Fabry et al., 1997). This method to retrieve the refractivity is based on phase measurements, in particular, on measurements of phase variation between responses from different stationary targets at different instants of time and has the advantage of being able to achieve high spatial and temporal resolution over flat terrain. The aim of this work is to analyze the statistical properties of radar estimates of the atmospheric refractivity. Results obtained over mountainous terrain will be discussed taking into account the height variation between the selected targets whose paths might be misaligned and the possible vertical variation of the atmospheric refractivity. The polarimetric weather radar data provided by the C-Band radar (Vaisala WRM200) of Meteogalicia located in Monte Xesteiras over mountainous terrain (Galician Region, Spain) will be used with the proposed algorithm to estimate refractivity and to analyze its statistical properties.

2. Retrieval of Refractivity from Phase Measurements: Theory Review

The refractive index n is defined as the ratio of the speed of the light in the vacuum to the speed of the light in any other medium. In the lowest part of the atmosphere, its value is slightly higher than 1 and its variations are of the order of 10^{-5}. Consequently, a deriver parameter, referred to as refractivity N, is commonly used and is defined as N=10^6·(n-1). The refractivity depends on three meteorological parameters such as the air pressure, the temperature and the water vapor pressure and is related to them through the following expression:

$$N = 77.6 \frac{p}{T} + 3.73 \cdot 10^5 \frac{e}{T^2} \tag{2.1}$$

where p is the air pressure (hPa), T is the absolute air temperature (K) and e is the water vapor pressure (hPa) which is obtained from the relative humidity (Bean and Dutton, 1968).

Following the algorithm proposed by (Fabry et al., 1997) and extended in (Fabry, 2004), the refractivity can be estimated from radar measurements, in particular, from phase measurements of backscattered signals from stationary ground targets. Furthermore, the mean refractivity change can be directly retrieved between the radar and the target when the temporal resolution is high enough to neglect the occurrence of phase wrapping. Mean refractivity changes with time can also be estimated between two stationary targets aligned with the radar. In this case, the mean refractivity variation between two different targets and two instants of time can be obtained as:

$$\Delta N(\Delta_r, \Delta_t) = -\frac{c}{4\pi f \Delta_r} 10^6 \Delta(\Delta\phi(\Delta_r, \Delta_t)) \tag{2.2}$$

where f is the radar frequency (5.6 GHz), Δ_r is the range between the targets (m), c is the speed of light in the vacuum ($3 \cdot 10^8 \ ms^{-1}$) and $\Delta(\Delta\phi(\Delta_r, \Delta_t))$ is the phase variation between the two targets at two different times. For a temporal resolution of 5 minutes, corresponding to the time between two consecutive PPI scans, considering a C-Band wavelength $\simeq$ 5.35 cm, the phase change between the two measurements varies approximately at a rate of $13.45°/km^{-1}$ for a variation in N of 1 unit.

3. Statistical Characterization of the Received Signal

The voltage of the received radar signal at time t in the k-th resolution cell can be written as the integral of the multiple backscattered elementary echoes in the resolution volume of each cell and can be expressed as:

$$V(r_k, t) = \int_v S(v, t) e^{-j\frac{4\pi}{\lambda}\int_0^{r(v)} n(r_k, t)dr} dv \tag{3.1}$$

where $S(v, t)$ is the complex backscattered amplitude from each differential volume within the resolution volume and $r(v)$ is the path travelled by the wave between the radar and every point in the resolution volume.

Within the resolution volume it is possible to find different classes of targets. Completely stationary targets are those that do not vary their scattering behavior with time. Non stationary targets vary with time and so vary their backscattered amplitude and phase. The backscattering from non stationary targets can vary very slow or very fast with time, depending on the correlation time of the target.
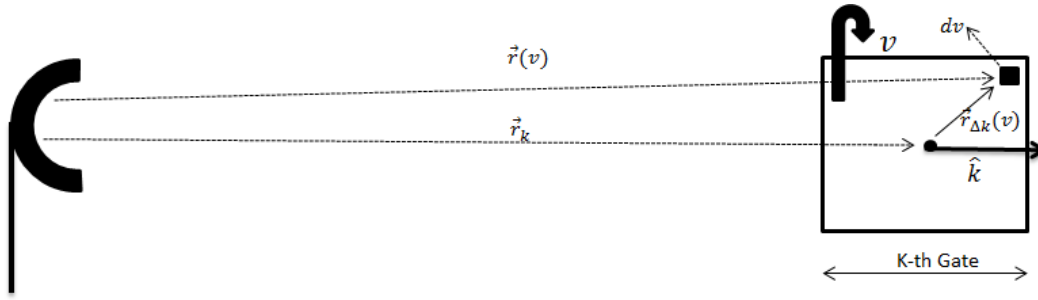

Figure 1: Scheme of the path travelled by the wave.

Scattering from ground targets is, in most cases, statistically well characterized by a complex circular Gaussian process. If only non-stationary targets are found within the resolution volume, then the process has zero mean, it is characterized in terms of the autocorrelation function or its corresponding Doppler spectrum, whose width will be narrow for targets slowly varying with time and wide for fast varying targets. Completely stationary targets will modify the mean of the process, which will differ from zero.

Let $X = [X_{11}, X_{12}, ..., X_{1N}, X_{21}, X_{22}, ..., X_{2N}]$ denote a 2N-dimensional vector of received voltage measurements, where the measurement $\mathbf{X_{kl}}$ corresponds to the k-th scan and the l-th pulse within that scan. The probability density function can be expressed as

$$f_{\theta_N}(\mathbf{x}) = (\mathbf{2\pi})^{\mathbf{N}} |\mathbf{R}|^{-\frac{1}{2}} \mathbf{e}^{-\frac{1}{2}(\mathbf{x}-\mathbf{m}(\theta_\mathbf{N}))^* \mathbf{R}^{-\mathbf{1}}(\theta_\mathbf{N})(\mathbf{x}-\mathbf{m}(\theta_\mathbf{N}))} \tag{3.2}$$

where $m(\theta_N) = \begin{bmatrix} ae^{j\theta} \\ ... \\ ae^{j\theta} \\ ae^{j(\theta+\theta_N)} \\ ... \\ ae^{j(\theta+\theta_N)} \end{bmatrix}$ is the 2N × 1 mean vector and $R(\theta_N) = \begin{bmatrix} R_{11}(N\times N) & R_{12}(N\times N)e^{j\theta_N} \\ R_{12}^*(N\times N)e^{-j\theta_N} & R_{11}(N\times N) \end{bmatrix}$ is the 2N × 2N

covariance matrix. The mean of the vector is determined by the completely stationary target backscattering. Its amplitude a is constant with time. For its phase, it is assumed constant during a scan, while it may change because of refractivity changes between scans. Therefore, θ is the phase measured at first scan and θ_N is the phase increment measured at the second scan, which is supposed to be due only to refractivity changes. This is therefore the parameter of interest for refractivity retrieval. Non stationary targets within the resolution volume will make the measurements noisier. Though their backscattering do not affect the mean, it will determine the covariance matrix. The covariance matrix elements in the diagonal are all equal to the mean power from the non-stationary targets. As a first approximation it will be assumed that non-stationary targets are uncorrelated in time so the covariance matrix is purely diagonal.

In this case, obtaining the maximum likelihood estimate of θ_N is straightforward (Kay, 1993):

$$\theta_N = arctg(\frac{\Im(\sum_{k=1}^N X_{2k})}{\Re(\sum_{k=1}^N X_{2k})}) - \theta; \qquad \theta = arctg(\frac{\Im(\sum_{k=1}^N X_{1k})}{\Re(\sum_{k=1}^N X_{1k})}) \tag{3.3}$$

4. Measurements of phase variation

4.1. Radar Data

Data were obtained from I/Q samples of radar returns with the C-Band Polarimetric Weather Radar of Meteogalicia located to the northwest of Spain (Galician Region) to 750 m (asl) over a complex terrain as shown the Fig. 2. The radar was configured

to perform continuous scan over an azimuth angle of 146.1° and an elevation angle of 0° with a pulse repetition frequency (PRF) of 900 Hz that leads to a temporal resolution of 1.1 ms. The spatial resolution between consecutive gates is 300 m and its beam width is approximately 1°. The radar data were collected on March 12, 2014, on a clear day and with weak wind (approximately 8.03 km/h). The reference time is at 09:47 UTC.

As a consequence of the very high temporal resolution scanning the same direction, the probability that the wrapping phase is minimum and so the error of the refractivity estimation decreases too.
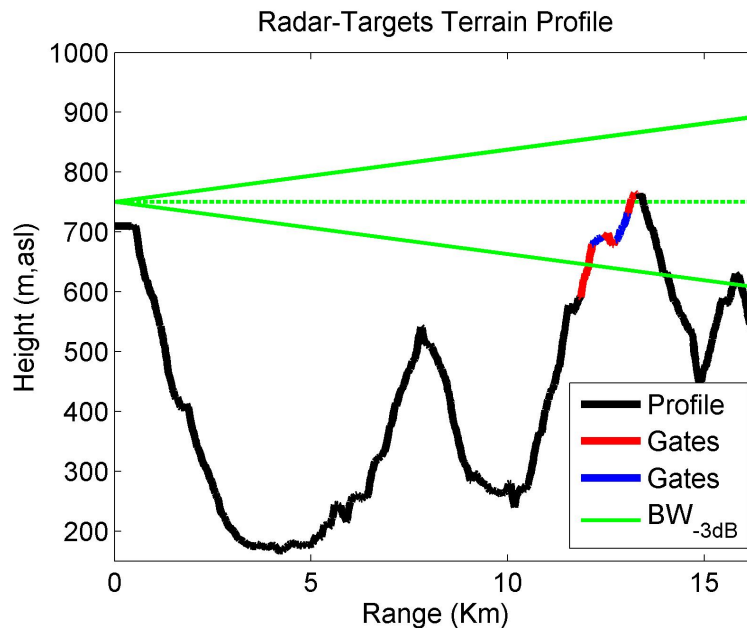

Figure 2: Profile between the radar and the targets. The red and blue lines represent 5 consecutive stationary gates. The green lines represent the theoretical BW_{-3dB} of the radar antenna.

4.2. Analysis of the uncertain sources

The Fabry algorithm allows estimating the average refractivity between two stationary targets over flat terrain, i.e., when the radar and the targets are aligned in the same path. Fig. 3 shows several stationary targets, which will exhibit highly correlated phases in time and one non-stationary targets (the one corresponding to gate #89) which will present completely uncorrelated phases in time.
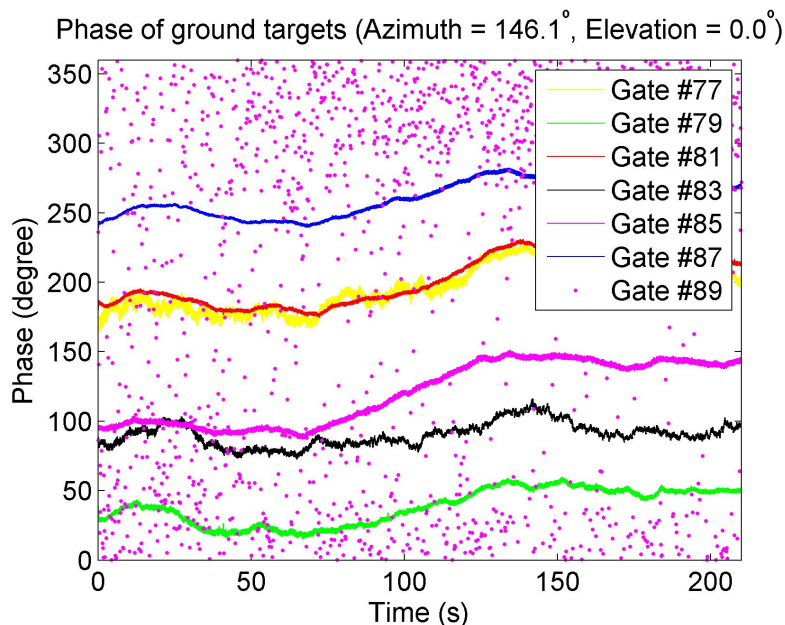

Figure 3: Phase of radar returns. The six first gates can be considered stationary targets because they exhibit correlated highly phases in time while the last gate is considered non-stationary target because it presents completely uncorrelated phase in time. The gates are located at ranges of 11.55, 11.85. 12.15, 12.45, 12.75 13.05 and 13.35 km from radar, respectively.

Nevertheless, the terrain profile used in this work is very mountainous, consequently, each target is possibly located at different heights and the estimated phase will be very noisy as can be seen in the Fig. 4 where the maximum likelihood estimate obtained in the previous section is used.
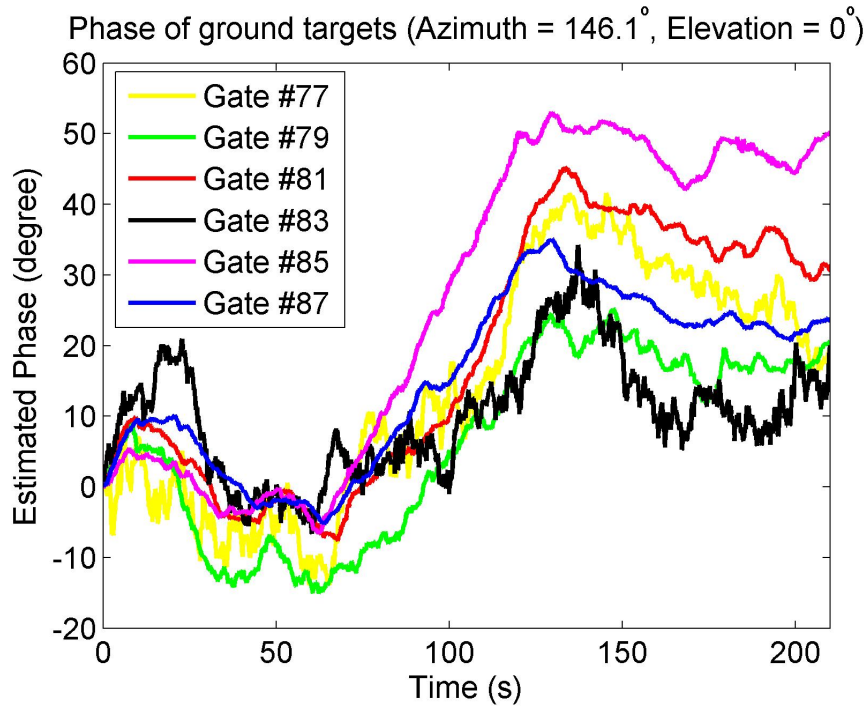

Figure 4: MLE of the phase from radar returns.

To properly analyze the phase increments obtained it will be neccessary to account not only for temporal variations of the refractivity, but also for time variations of the gradient refractivity, and specially for the variation of refractivity with height.

$$\Delta N(\Delta_r, \Delta_t) = \Delta N_0(\Delta_r, \Delta_t) + \Delta h(\Delta_r) \cdot \Delta(\frac{\partial N(\Delta_r, \Delta_t)}{\partial h}) \tag{4.1}$$

The first term on the right-side represents the average refractivity variation considering that the targets are located at the same height as the radar while the second term represents refractivity variations due to the height variations of the targets with respect to the radar and due to changes in the propagation conditions such as the vertical gradient of the refractivity ($\frac{\partial n}{\partial h}$) considering further the ray curvature relative to the Earth curvature (Park and Fabry, 2010). The contribution of each term to the estimated phase variation is analyzed in detail below:

1. The horizontal variation of the refractivity.

   Taking into account that the distance between two consecutive cells (300 m) is much shorter than the whole path length (between 11.55 and 13.35 km), the averaged refractivity variation between two nearby gates in a short instant of time will be minimum and will not reach half a degree. The horizontal refractivity variation in a specific cell should be very higher with respect to the previous gates to find meaningful changes in the average refractivity along path. Moreover, the averaged refractivity variation is the parameter to be retrieved in the Fabry algorithm.

2. The height variation of the targets with respect to the radar associated with the vertical gradient of the refractivity ($\partial n/\partial h$).

   The higher phase variations are caused by this term. A slight variation of the vertical gradient of the refractivity may cause a strong variation between the phases if the targets are highly misaligned. For range around 13 km and for a beam width of $1°$, the height variation between targets in consecutive cells could even be up to 200 m. Over the profile presented in Fig. 2, it is possible to find a height variation between targets around 100 m for any consecutive cells.

3. The ray curvature relative to the curvature of the Earth.

   This term depends on the curvature of the ray path related to the Earth curvature and the path length variations due to changes of the vertical gradient of the refractivity. It does not depend on height of the targets and, consequently, the phase variation is practically null.

Additionally, another error source is the standard deviation of the phase difference, $\sigma_{1,2}$, between two returns. If the phase distributions of each target $\sigma_i(t)$ are considered temporarily independent and identically distributed, the standard deviation of

the temporal phase variation $\Delta\phi = \phi(t_1) - \phi(t_0)$ is:

$$\sigma_{\Delta\phi} = \sqrt{\sigma_{\phi(t_1)}^2 + \sigma_{\phi(t_0)}^2} = \sqrt{2}\sigma_\phi \qquad (4.2)$$

and then, the standard deviation of the spatial phase variation $\Delta(\Delta\phi) = \Delta\phi(r_1) - \Delta\phi(r_0)$ is :

$$\sigma_{1,2} = \sqrt{2} \cdot \sigma_{\Delta\phi} = 2 \cdot \sigma_\phi \qquad (4.3)$$

4.3. Numerical Results

Taking into account the gates #85 and #87, located approximately at 720 and 790 m (asl) respectively, as the most stationary targets with higher backscattered power, a standard vertical gradient of reference of -40 ppm km^{-1} and a representative vertical gradient variation of the refractivity of 1 N-unit between the reference time and the measured time, the phase variation between both gates due to height variation could be up $8.67°$ causing a phase variation very noisy while the contribution of the ray curvature variation is only $0.0136°$.

Furthermore, considering a conservative standard deviation of $2°$ in stationary targets, the maximum standard deviation of the phase variation $\Delta(\Delta\phi)$ is about $4°$ and it will be the main error source when the targets are aligned with the radar or when the vertical gradient variation is minimum as can be seen in the first row in the table I.

The estimation of each error source in function of the terms analyzed in the equation 4.1 and the variance of the phase of the returns are summarized in the table I for different vertical gradient variations, where the estimated phase variation matches with the phase variation between the targets #85 and #87 in Fig. 4 when the vertical gradient variation is about 2 N-units.

Table 1: Phase variation in function of each term of equation 4.1.

$\Delta(\frac{\partial n}{\partial h})(N-units)$	Standard Deviation	Height (°)	Curvature (°)	Total (°)
0.1	4.0	0.86	0.0013	5.07
1	4.0	8.67	0.0136	12.89
2	4.0	17.35	0.0275	21.58
3	4.0	26.02	0.042	30.27

5. Conclusions and Future Work

In this work, the maximum likelihood estimate of the phase variation is obtained assuming one completely stationary target and non-stationary targets uncorrelated in time. Hence, the covariance matrix is purely diagonal and the estimate is easily obtained. Nevertheless, a resolution cell can have an unknown number of completely stationary targets and non-stationary targets varying slowly with time causing that the matrix covariance is not diagonal and the amplitude of the mean of the vector is variable and therefore the maximum likelihood estimate is more complicated.

Furthermore, the noisiness of estimated phase measurements due to different sources of uncertainty such as the height variations between the targets, the position of the target in a resolution cell or changes in the vertical gradient of the refractivity are quantified to obtain a more accurate estimation of the refractivity. The largest sources of noisiness will be due mainly to the change in the vertical gradient of the refractivity together with the height variation of the targets reaching variations about $8.6°$ for vertical gradient variations of 1 N-unit and height variations about 70 m.

Future works will be based on estimating the phase of the backscattered signal taking into account various completely stationary targets and non-stationary targets within the same resolution cell. In addition, future works will be focused on estimating, as precisely as possible, the phase taking into account height variations of the targets and variations in the vertical gradient of the refractivity. A time series of refractivity measurements over a longer period will be used to analyze the statistical characterization to long term.

Acknowledgement

References

B. R. Bean and E. J. Dutton, "Radio meteorology," in *New York: Dover*, June 1968.

O. T. Davies, C. N. Mitchell, P. S. Spencer, J. D. Nash, and R. J. Watson, "Application of gps phase delay measurements in radio science and atmospheric studies," in *IEE Proc. Microwave Antennas Propagation*, vol. 151, February 2004.

F. Fabry, "Meteorological value of ground target measurements," in *Journal Atmospheric and Oceanic Technology*, vol. 21, April 2004, pp. 560–573.

F. Fabry, C. Frush, I. Zawadzki, and A. Kilambi, "On the extraction of near-surface index of refraction using radar phase measurements from ground targets," in *Journal Atmospheric and Oceanic Technology*, vol. 14, August 1997, pp. 978–987.

S. M. Kay, "Fundamentals of statistical signal processing: Estimation theory," in *Prentice Hall Signal Processing Series*, 1993.

S. Park and F. Fabry, "Simulation and interpretation of the phase data used by radar refractivity retrieval algorithm," in *Journal Atmospheric and Oceanic Technology*, vol. 27, August 2010, pp. 1286–1301.

Y. Selén and J. Kronander, "Optimizing power limits for white space devices under a probability constraint on aggregated interference," in *IEEE International Symposium on Dynamic Spectrum Access Networks (DYSPAN)*, June 2012.

M. Viher, T. Kos, and I. Markevic, "A study of the maximal height for the exponential model of the refractivity index vertical profile in the republic of croatia," in 53th *International Symposium (ELMAR)*, September 2011.

R. J. Watson and C. J. Coleman, "The use of signals of opportunity for the measurement of atmospheric refractivity," in *IEEE International Geoscience and Remote Sensing Symposium (IGARSS)*, July 2012.

C. L. Ziegler, T. J. Lee, and R. A. Pielke, "Convective initiation at the dryline: A modeling study," in *Mon. Weather Rev.*, vol. 125, June 1997, pp. 1001–1026.